DE GRUYTER OPEN

Chemical and Process Engineering 2017, 38 (1), 31-50
DOI: 10.1515/cpe-2017-0004

PAN

ESTIMATION OF FILTRATION EFFICIENCY – FROM SIMPLE CORRELATIONS TO DIGITAL FLUID DYNAMICS

Rafał Przekop*

Warsaw University of Technology, Faculty of Chemical and Process Engineering, ul. Waryńskiego 1, 00-645 Warsaw, Poland

Dedicated to Prof. Leon Gradoń on the occasion of his 70th birthday

Aerosol filtration in fibrous filters is one of the principal methods of accurate removal of particulate matter from a stream of gas. The classical theory of depth filtration of aerosol particles in fibrous structures is based on the assumption of existing single fibre efficiency, which may be used to recalculate the overall efficiency of entire filter. Using "classical theory" of filtration one may introduce some errors, leading finally to a discrepancy between theory and experiment. There are several reasons for inappropriate estimation of the single fibre efficiency: i) neglecting of short-range interactions, ii) separation of inertial and Brownian effects, ii) perfect adhesion of particles to the fibre, iv) assumption of perfect mixing of aerosol particles in the gas stream, v) assumption of negligible effect of the presence of neighbouring fibres and vi) assumption of perpendicular orientation of homogenous fibres in the filtration structure. Generally speaking, "classical theory" of filtration was used for characterization of the steady – state filtration process (filtration in a clean filter, at the beginning of the process) without deeper investigation of the influence of the nternal structure of the filter on its performance. The aim of this review is to outline and discuss the progress of deep-bed filtration modelling from the use of simple empirical correlations to advanced techniques of Computational Fluid Dynamics and Digital Fluid Dynamics.

Keywords: filtration, lattice Boltzmann, Brownian dynamics, multi-phase flows, porous media

1. INTRODUCTION

A collection of aerosol particles in the particular steps of their production, and purification of the air at the workplace and atmospheric environment requires an efficient separation method of particulate matter from the carrier gas. Filtration is one of the most effective methods of particle removal from an aerosol stream. New fibrous structures could provide a promising tool for the development of highly efficient filters. A fibrous material operates by capturing an aerosol particle on fibre surface within the filter depth. Its effectiveness depends on the particle and fibre size, filter porosity and material properties of particle and filter media. Performance of a filter can be defined by its efficiency, pressure drop, and dust capacity. The basic principle of deep bed filtration is that solid particles suspended in a fluid are typically smaller than the pores of the filtering medium and as they deposit on fibres they become evenly distributed in the entire volume of the filter. As the fluid-solid suspension flows through the filter, particles present in the suspension deposit at various depths within the bed, that is, on solid walls bordering pore spaces. This leads to progressive clogging of a filter and a subsequent increase of pressure drop across it. Thus, it is usual to divide the filtration process into two stages: initial and aging. In the initial stage, the deposition of particles inside the filter is relatively small. Its effect on the

*Corresponding author, e-mail: r.przekop@ichip.pw.edu.pl

Unauthenticated
Download Date | 12/15/17 11:50 AM

properties of the filter is negligible, and the performance of the filter can be regarded as that of a clean filter.

However, to produce the optimal filter structure for the given application, it is necessary to know not only the characteristic of a clean filter but also its behaviour during loading. The presence of previously deposited particles causes an increase of both – filtration efficiency and pressure drop. It is worth noting that not only the total amount of deposited particles but also their spatial distribution and structure affect filter performance. When pressure drop approaches the maximum acceptable value that corresponds to the clogging of the media the filter has to be regenerated or changed.

The application of the "classical theory" of filtration for description of filter performance may introduce some errors for the realistic filter behaviour. There are several reasons for inappropriate estimation of the single fibre efficiency: neglecting of short-range interactions, separation of inertial and Brownian effects in description of particle motion, assumption of perfect adhesion of particles to the fibre and perfect mixing of aerosol particles in the gas stream, assumption of negligible effect of the presence of neighbouring fibres and their perpendicular orientation in the filtered structure.
The aim of this review is to outline and discuss the progress of deep-bed filtration modelling from the use of simple empirical correlations to advanced techniques of Computational Fluid Dynamics and Digital Fluid Dynamics.

2. CLASSICAL THEORY OF DEEP BED FILTRATION

The main assumptions of "classical theory" can be summarised as follows (Podgórski, 2002):

- Initial penetration of aerosol particles through a filter is calculated as:

$$1-\eta = exp(-\lambda L) \tag{1}$$

- The filter coefficient is related to single fibre efficiency as:

$$\lambda = \frac{4E}{\pi d_F}\left(\frac{1-\varepsilon}{\varepsilon}\right) \tag{2}$$

- The single fibre efficiency (defined as a ratio of the flux of particles depositing onto the fibre to the flux of particles passing a surface being projection of the fibre onto a plane perpendicular to the direction of mean motion) is calculated assuming that the deposition efficiency due to deterministic mechanisms (inertial impaction, sedimentation, electrostatic force) and stochastic mechanism (Brownian diffusion) are independent:

$$E = 1-(1-E_{det})(1-E_{diff}) \tag{3}$$

- E_{det} may be obtained using limiting trajectory concept and solving the deterministic, Lagrangian equation of motion for a particle, neglecting Brownian motion, E_{diff} is calculated solving Eulerian (convective-diffusion) equation for a weightless particle in the absence of external forces.
- Both, E_{det} and E_{diff} are calculated for an assumed model of gas flow around a single circular fibre.
- The perfect adhesion. No rebound of a particle colliding with fibre surface may occur.

3. GAS FLOW MODELS

3.1. Isolated fibre models

The existing models of gas flow in fibrous filters were developed in most instances for the 2D case. For isolated fibre models, the gas flow field near a collector in a fibrous filter is estimated solving the governing equations for the simplest geometrical system of a single, circular cylinder in unbounded

Unauthenticated
Download Date | 12/15/17 11:50 AM

space. Consequently, the effect of neighbouring fibres on the gas flow pattern around the fibre considered is completely neglected.

The potential flow was the first model ever used to investigate aerosol filtration in fibrous filters theoretically (Albrecht, 1931; Sell, 1931). The potential flow is the model of a steady state, vorticity-free flow of an inviscid, incompressible fluid. The major drawbacks of the potential flow model are related to the neglect of the fluid viscosity and the assumption of zero vorticity due to which the tangential component of the gas velocity does not vanish at the fibre surface. Consequently, gas velocities are much too high near the fibre and hence the efficiency of aerosol particle deposition calculated using this model is expected to be significantly overestimated.

As most fibrous filters operate at low Reynolds numbers defined as $Re = U\, d_f / \nu_f$, the model of creeping flow seems to be a much better alternative than that of potential flow. This approximation assumes predomination of the viscous forces over the inertial ones. Unfortunately, it is impossible to match the constants of integration in order to satisfy exactly all the boundary conditions (fixed velocity in infinity and vanishing gas velocity at the fibre surface).

The validity of the creeping flow approximation that neglects the inertial effects of the fluid motion is restricted to the values of the Reynolds number below about 0.5; losing a bit more accuracy it could be extended to $Re = 1$. An approximate method of approach to this issue enabling an analytical solution to the problem was suggested by Oseen (1927). The first approximate solution to that problem for the transverse flow past a circular cylinder was given by Lamb (1932). Two important features of the Lamb model should be outlined: being formally a solution to the Oseen problem, it still retains the downstream-upstream symmetry, so that the inertial effects of the fluid flow are not accounted for properly, and although the gas velocity vanishes at the fibre surface, both components of the velocity tend to infinity far from the fibre. It means that the Lamb model is still limited to very low values of the Reynolds number. But in addition, the Lamb model might have a high degree of error if used in the modelling of filters with extremely high porosity, when the mean inter-fibre distances are very large compared to the fibre diameter and one has to compute the trajectories of aerosol particles beginning very far from the fibre.

The next, more successful trial to improve the Lamb solution, was undertaken by Tomotika and Aoi (1950) who employed a different kind of expansion to obtain the stream function as a sum of the stream function given by Lamb plus a correction term proportional to the Reynolds number. Tomotika and Aoi's solution is a first order (with respect to Re) correction to the Lamb model, hence it also possesses an undesirable property of diverging gas velocity to infinity at an infinite distance from the fibre, though, like for the Lamb model, the non-slip conditions at the fibre surface are fulfilled exactly. Podgórski (1993) has shown a very accurate solution to the Oseen problem using Imai's (1951) method of a complex disturbance velocity. A comprehensive comparison of the various flow models past an isolated fibre and an analysis of their applicability in the modelling of aerosol filtration in fibrous filters was presented by Lastow and Podgórski (1998).

3.2. Fibre in cell models

In contrast to isolated fibre models, fibre-in-cell models also describe one fibre but it placed centrally in a finite volume of fluid, called the unit cell. For the most popular, Kuwabara (1959) and Happel (1959) models, this unit cell is a cylinder (coaxial with a fibre) of radius R_K , such that $R_K = R_c / \alpha^{1/2}$, Kuwabara (1959) derived a formula for the stream function for the creeping flow assuming non-slip conditions on the fibre surface and normal velocity and vorticity at the border of the unit cell to be zero. Happel (1959) obtained a similar solution assuming the tangential stress instead of vorticity to be zero at the cell border.

Unauthenticated
Download Date | 12/15/17 11:50 AM

Kirsch and Fuchs (1967) measured fluid velocities in a system of parallel cylinders and concluded that the Kuwabara formula fits the experimental data better than the Happel solution. The Kuwabara model was extended by Pich (1966), Yeh and Liu (1974) and Henry and Ariman (1981) to allow for possible gas slip on the surface of an ultrathin fibre. In practice, this extension is important for fibres with a diameter below one micrometer. A disadvantage of the Kuwabara and Happel models is related to the fact that it is impossible to compose a filter structure as a set of circular unit cells (without the cells overlapping or empty spaces between them). Marshall et al. (1994) derived an approximate analytical solution for a fibre in a square cell that obeys periodic boundary conditions; the resulting formula for the stream function is much more complex than the Kuwabara solution. The authors reported that deposition efficiency predicted by the rectangular cell model is higher than that for the original Kuwabara model. Banks and Kurowski (1990) extended the 2D Kuwabara model for the case of gas flow past a fibre inclined with respect to the main direction of the gas flow.

3.3. Analytical solution of flow around two fibres

Przekop and Podgórski (2004) have proposed a solution to the Oseen problem for the case of two cylindrical fibres. The authors noticed that an approximate analytical solution can easily be obtained using Imai's (1951) method of complex disturbance velocity, which was used earlier by Podgórski (1993) to obtain a solution to the Oseen problem in case of a single fibre. Let us introduce two Cartesian coordinate systems Ox_1y_1- and Ox_2y_2- engaged in the centre of the second fibre, oriented such that axes Ox_1 and Ox_2 overlap the main direction of gas flow. Similarly, let us introduce two cylindrical coordinate systems engaged in the centre of both fibres, $Or_1\theta_1$ and $Or_2\theta_2$, where angles θ_1 and θ_2 are measured from axes Ox_1 and Ox_2, respectively, counter-wise to the main direction of the gas flow (Fig. 1).

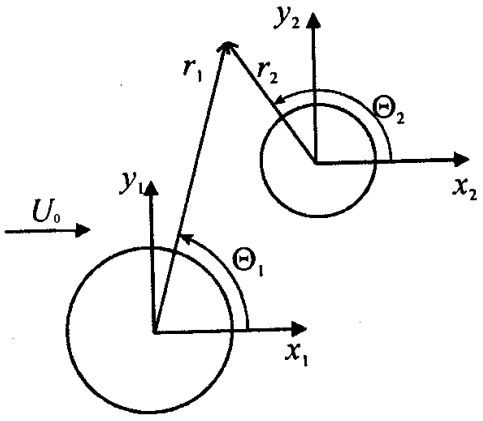

Fig. 1. Definition of the co-ordinates systems for flow past two fibres

Following the Imai's scheme one may introduce a complex coordinate $z = x + iy$, where $i = \sqrt{-1}$ is an imaginary unit and a complex disturbance velocity U, such that $U+u_0=u_x-iu_y$. A general solution to the Oseen problem in cylindrical coordinate system has the following form if one decomposes U into harmonic, U_h, and non-harmonic, U_u, components:

$$U = U_h + U_u = \sum_{i=1}^{\infty} \frac{A_n}{r_n} exp(-in\theta) + \\ + exp(k^* x) \sum_{i=1}^{\infty} [B_n K_{n-1}(k^* r) exp[i(n-1)\theta] + \overline{B}_n K_n(k^* r) exp(-in\theta)] \tag{4}$$

cpe.czasopisma.pan.pl; degruyter.com/view/j/cpe
Unauthenticated
Download Date | 12/15/17 11:50 AM

where

$$k^* = \frac{U}{2\nu} \tag{5}$$

Let us define:

$$\begin{aligned} A_n &= a_n + i\alpha_n \\ B_n &= b_n + i\beta_n \\ \overline{B}_n &= b_n - i\beta_n \end{aligned} \tag{6}$$

In view of $u_x = u_0 + Re(U)$ and $u_y = Im(U)$, where $Re(U)$ and $Im(U)$ denote the real and imaginary parts, respectively, we can calculate their values as:

$$\begin{aligned} u_x = u_0 &+ \sum_{n=1}^{N} \frac{a_n^{(1)} \cos n\theta_1 + a_n^{(1)} \sin n\theta_1}{r_1^{\,n}} + \sum_{n=1}^{N} \frac{a_n^{(2)} \cos n\theta_2 + a_n^{(2)} \sin n\theta_2}{r_2^{\,n}} + \\ &+ \exp(k^* x_1) \sum_{n=1}^{N} b_n^{(1)} [K_{n-1}(k^* r_1) \cos(n-1)\theta_1 + K_n(k^* r_1) \cos n\theta_1] + \\ &- \exp(k^* x_1) \sum_{n=1}^{N} \beta_n^{(1)} [K_{n-1}(k^* r_1) \sin(n-1)\theta_1 + K_n(k^* r_1) \sin n\theta_1] + \\ &+ \exp(k^* x_2) \sum_{n=1}^{N} b_n^{(2)} [K_{n-1}(k^* r_2) \cos(n-1)\theta_2 + K_n(k^* r_2) \cos n\theta_2] + \\ &- \exp(k^* x_2) \sum_{n=1}^{N} \beta_n^{(2)} [K_{n-1}(k^* r_2) \cos(n-1)\theta_2 + K_n(k^* r_2) \cos n\theta_2] \end{aligned} \tag{7}$$

$$\begin{aligned} -u_y = &\sum_{n=1}^{N} \frac{a_n^{(1)} \cos n\theta_1 - a_n^{(1)} \sin n\theta_1}{r_1^{\,n}} + \sum_{n=1}^{N} \frac{a_n^{(2)} \cos n\theta_2 - a_n^{(2)} \sin n\theta_2}{r_2^{\,n}} + \\ &+ \exp(k^* x_1) \sum_{n=1}^{N} b_n^{(1)} [K_{n-1}(k^* r_1) \sin(n-1)\theta_1 - K_n(k^* r_1) \sin n\theta_1] + \\ &+ \exp(k^* x_1) \sum_{n=1}^{N} \beta_n^{(1)} [K_{n-1}(k^* r_1) \cos(n-1)\theta_1 - K_n(k^* r_1) \cos n\theta_1] + \\ &+ \exp(k^* x_2) \sum_{n=1}^{N} b_n^{(2)} [K_{n-1}(k^* r_2) \sin(n-1)\theta_2 - K_n(k^* r_2) \sin n\theta_2] + \\ &+ \exp(k^* x_2) \sum_{n=1}^{N} \beta_n^{(2)} [K_{n-1}(k^* r_2) \cos(n-1)\theta_2 - K_n(k^* r_2) \cos n\theta_2] \end{aligned} \tag{8}$$

To obtain $8N$ constants of integration ($a_n^{(1)}$, $b_n^{(1)}$, $a_n^{(2)}$, $b_n^{(2)}$, $\alpha_n^{(1)}$, $\beta_n^{(2)}$, $n = 1,\ldots, N$) one uses the zero-velocity condition for both components on both fibre surfaces and expands the exponential components into Fourier-Bessel series which leads to a system of $8N$ linear equations, from which the necessary constants may be derived.

Similary to Podgórski (1993) solution for the case of a single fibre, the method fulfils the condition of steady gas velocity away from the fibre surface.

The results obtained by Przekop and Podgórski (2004) have shown a strong influence of mutual fibre orientation on filtration efficiency and spatial distribution of deposits, which suggests that mesoscale

Unauthenticated
Download Date | 12/15/17 11:50 AM

inhomogeneity of filter structures may influence the overall filtration efficiency. This problem will be discussed later in this review.

3.4. Multi fibre models

No exact analytical solution to the problem of gas flow in a system consisting of many fibres exists. However, some analytical approximate solutions can be obtained for assumed regular arrangements of fibres. There are two popular models of a fibrous filter: channel structure (rectangular array) and staggered model (hexagonal array). The basic element of such structures is a row of parallel cylinders. General solutions of the problem of creeping flow past a row of fibres were obtained by Tamada and Fujikawa (1957) and Miyagi (1958) in the form of an infinite series. Explicit expressions for gas velocity components taking into account only the first terms of the series were first presented by Kirsch and Stechkina (1977). However, such a description was not sufficiently accurate (for typical values of the filter porosity, that solution gave the velocity on the fibre surface of the order of 10% of the mean gas velocity). Expansions for two terms of the series were given by Podgórski and Gradoń (1992), and an even more accurate solution for three terms was presented by Podgórski et al. (1998).

4. THE COUPLING OF DETERMINISTIC AND STOCHASTIC MECHANISMS

Particle collection by interception occurs when a particle follows a gas streamline that happens to come within a particle radius to the surface of a fibre. The particle hits the fibre and is captured due to its finite size. The single fibre deposition efficiency due to interception depends on the dimensionless parameter, R, defined as

$$R = \frac{d_p}{d_F} \tag{9}$$

The single fibre efficiency due to interception was given by Lee and Ramamurthi (1993) as:

$$E_R = \frac{(1-\alpha)R^2}{Ku(1+R)} \tag{10}$$

where Kuwabara factor, Ku, is defined as:

$$Ku = -\frac{ln\,\alpha}{2} - \frac{3}{4} + \alpha - \frac{\alpha}{4} \tag{11}$$

Inertial impaction occurs when the particle, because of its inertia, is unable to adjust quickly to the abruptly changing streamlines near the fibre and crosses those streamlines to hit the fibre. The parameter that governs this mechanism is Stokes number

$$Stk = \frac{\rho_p d_p C_c U}{18 \mu d_F} \tag{12}$$

The single fibre efficiency for inertia was given by Yeh and Liu (1974)

$$E_I = \frac{Stk\ J}{Ku^2} \tag{13}$$

where:

$$J = \left(29.6 - 28\alpha^{0.62}\right)R^2 - 27.5R^{2.8} \qquad \text{for } R < 0.4$$

$$J = 2.0 \qquad \text{for } R > 0.4 \tag{14}$$

cpe.czasopisma.pan.pl; degruyter.com/view/j/cpe
Unauthenticated
Download Date | 12/15/17 11:50 AM

Impaction is the most important mechanism for large particles. But such particles reveal significant collection by direct interception as well. The sum of E_I and E_R may not exceed the theoretical value of R+1.

The Brownian motion of small particles is sufficient to greatly enhance the probability of their hitting a fibre while travelling past it on a non-intercepting streamline. The single fibre efficiency is a function of dimensionless Peclet number, Pe

$$Pe = \frac{d_F U}{D} \tag{15}$$

The single fibre efficiency due to diffusion was empirically determined by Kirsch and Fuchs (1968) as

$$E_{diff} = 2Pe^{-2/3} \tag{16}$$

Theoretical expression for E_{diff} including the effect of Ku was presented by Brown (1993)

$$E_{diff} = 2.9\left(\frac{1-\alpha}{Ku}\right)^{1/3} Pe^{-2/3} + 0.62Pe^{-1} \tag{17}$$

In estimating the deposition efficiency near the size of minimum efficiency Hinds (1999) reported the necessity to include the interaction term for enhanced collection due to the interception of diffusing particles

$$E_{BD} = \frac{1.24R^{2/3}}{(KuPe)^{1/2}} \tag{18}$$

Generalised Brownian dynamics algorithm accounting simultaneously for particle inertia, random walk, convection in a moving fluid and influence of external forces was derived by Podgórski (2002) from Chandrasekhar's (1943) method. Particle trajectory is calculated for the generalised Besset-Boussinesqu-Ossen equation, which in a simplified form is reduced to the following expression:

$$m\frac{dv}{dt} = F^{(D)} + F^{(ext)} + F^{(R)} \tag{19}$$

Integration of Eq. (19) for the time interval Δt, small enough that the host fluid velocity u_i and the external force $F_i^{(ext)}$ may be assumed constant over $(t,t + \Delta t)$, gives the following bivariate normal density probability distribution functions $\varphi_i(\Delta v_i, \Delta L_i)$ that during time interval Δt the particle will change its i^{th} component of velocity by Δv_i and it will be displaced by a distance ΔL_i in i^{th} direction.

$$\varphi_i(\Delta v_i, \Delta L_i) = \frac{1}{2\pi\sigma_{vi}\sigma_{Li}\sqrt{1-\rho_c{}^2}} exp\left\{-\frac{1}{2(1-\rho_c)^2}\left[\left(\frac{\Delta v_i - <\Delta v_i>}{\sigma_{Li}}\right) - \right.\right.$$
$$\left.\left. - \frac{2\rho_c(\Delta v_i - <\Delta v_i>)(\Delta L_i - <\Delta L_i>)}{\sigma_{vi}\sigma_{Li}} + \left(\frac{\Delta L_i - <\Delta L_i>}{\sigma_{Li}}\right)^2\right]\right\} \tag{20}$$

The generalised algorithm for the Brownian dynamics can be formulated as follows. For a given initial particle position and its initial velocity components, v_i, at a moment t, we calculate the local fluid velocity, u_i, the external forces, $F_i^{(ext)}$, then, one calculates the expected values $<\Delta v_i>$ and $<\Delta L_i>$ and the correlation coefficient, ρ_c. Next, we generate two independent random values G_{Li}, G_{vi}, having Gaussian distribution with zero mean and a unit variance. Finally, we calculate the change of particle velocity, Δv_i, and the particle linear displacement, ΔL_i, during time step Δt from the expressions accounting for deterministic and stochastic motion:

Unauthenticated
Download Date | 12/15/17 11:50 AM

$$\Delta v_i = < \Delta v_i > + G_{vi}\sigma_{vi} \tag{21}$$

$$\Delta L_i = < \Delta L_i > + \rho_c G_{vi}\sigma_{Li} + \left(1-\rho_c{}^2\right) G_{Li}\sigma_{Li} \tag{22}$$

All the steps are repeated for each co-ordinate i = 1, 2, 3. Having determined the increments Δv_i and ΔL_i the new particle velocity at the moment $t + \Delta t$ is obtained as $v_i(t+\Delta t) = v_i + \Delta v_i$, and in the same manner the new particle's position is calculated. After completing one time-step of simulations, the next step is performed in the same way.

Based on comparison of Brownian dynamics calculations of a single fibre efficiency and "classical theory" estimations of deterministic and diffusive deposition, Sztuk et al. (2012) have reported the enhancement term in a similar form to Eq. (18).

5. THERMAL REBOUND AND RESUSPENSION

5.1. Empirical correlations

Most theories of aerosol filtration in fibrous filters assume that the particle is captured when it collides with a fibre. However, the particle may bounce-off the collector if its kinetic energy is high enough to overcome the energy of adhesion. Maus and Umhauer (1997) observed experimentally that the collection efficiency of particle drops for values of the Stokes number above 2. The authors suggested the following empirical correlation for the adhesion efficiency (defined as the ratio of the actually measured collection efficiency to that calculated with the particle rebound neglected):

$$AE = (1.76Stk)/\left(1+Stk^2\right) \tag{23}$$

Another formula was proposed by Ptak and Jaroszczyk (1990):

$$AE = 190/\left[190+\left(18\ Stk^2 d_F/d_p\right)^{0.68}\right] \tag{24}$$

Using the data collected by Brown (1993), Podgórski et al. (1998) derived another correlation:

$$AE = 1.8\times10^{-4} E_{kp}{}^{-0.24} \tag{25}$$

Kasper et al. (2010) have introduced bounce parameter $\beta \sim Stk/R$. The authors concluded that compact, forward facing deposit structures dominate in case of significant particle bounce ($\beta > \beta^*$ where β^* represents the critical conditions for the onset bounce on the bare fibre). For smaller values of bounce parameter, dendritic structures with pronounced sideways branching are formed. The critical bounce parameter is defined as $\beta^* = d_p U^*$. The critical fluid velocity, U^*, is defined as fluid velocity above which particles start to bound. Critical fluid velocity depends on particle size and material (Wang and John, 1987).

5.2. Molecular Dynamics

Moskal and Przekop (2002) have used Molecular Dynamics method to model particle deposition on surfaces. In this method the motion of each particle is computed by Newton's law. The standard pair-wise potential in Molecular Dynamics simulations is the Lennard-Jones potential

Unauthenticated
Download Date | 12/15/17 11:50 AM

$$\phi = -4\varepsilon_b \left[\left(\frac{\sigma}{r_a} \right)^6 - \left(\frac{\sigma}{r_a} \right)^{12} \right] \tag{26}$$

Molecular dynamics can be used to calculate, both, static and dynamic properties of the system. The method briefly described above was used to simulate the impact of a particle with collector surface. Particle deformations during the impact were observed. Also, the possibility of particle rebound from surface was theoretically confirmed. The method allows to predict forces acting between the particle and surface during the impact.

5.3. Energy-balanced oscillatory model

Energy-balanced oscillatory model of particle rebound and resuspension was introduced by Przekop et al. (2004). The model is based on adhesion theory. There are two dominating models of particle adhesion proposed by Johnson et al. (1971), known as JKR theory, and by Derjaguin et al. (1975), referred to as DMT theory. The JKR model assumes that adhesion-induced deformations are entirely elastic. Deformations could be calculated from three terms: the elastically stored energy from creating the contact zone, the mechanical potential energy, and the surface energy. The JKR theory assumes that interaction forces exist at the contact area only. When the applied load is negative, the contact area decreases. This means that the force of adhesion may be defined as the opposite of the force required to separate two bodies:

$$F_a = \frac{3}{2} \pi \gamma d_p \tag{27}$$

The contact area corresponding to this force is not zero. However, it jumps to zero as the surfaces spontaneously separate. The DMT theory does not approach the problem of particle adhesion from a contact mechanism perspective. It takes into account the molecular attraction in the noncontact zone. The analysis consists of two steps: determination of a shape of a particle near the contact surface and calculation of the sticking force. The applied load causes a pressure distribution over the contact area. The DMT model assumes that this distribution is given by Hertz equations (Hertz, 1896). The theory considers the generalised force of particle attraction, F_s, the elastic reaction force, F_e, and the adhesion force, $F_a = F_s - F_e$. When the sphere just touches the plane ("point contact"), there is no deformation and the adhesion force has the maximum value:

$$F_a = 2\pi \gamma d_p \tag{28}$$

Muller et al. (1980) proposed a model, later called MYD, in which the surface forces were calculated by doing a pairwise summation of interaction potentials between atoms. The basic assumption is that atoms in a particle are interacting with those in the substrate via a Lennard-Jones potential (Lennard-Jones, 1924) and the motion of one atom does not affect the position of neighbouring atoms. According to MYD theory, both the JKR and DMT models are its subsets and have their ranges of validity. The JKR model is proper for compliant materials, large particles, and high values of work of adhesion, whereas the DMT model is valid for small particles, more rigid materials, and lower surface energies.

The resuspension model is based on works by Reeks et al. (1988) and Ziskind et al. (2000). The authors assumed that the adhesion force and elastic reaction force considered in the JKR theory can be described by an equation of harmonic movement with dumping effect. Extending this approach, one can assume that the interactions between particles also have an oscillatory character. The displacement of a particle at the cluster attached to the neighbouring particles can be expressed as follows:

$$-kx - b\frac{dx}{dt} = m\frac{d^2x}{dt^2} \tag{29}$$

Unauthenticated
Download Date | 12/15/17 11:50 AM

The coefficient of stiffness can be calculated from the expression:

$$k = 2.4\left(\gamma\kappa^2 \frac{{d_p}^2}{4}\right)^{1/3} \tag{30}$$

The elastic constant κ is given by:

$$\kappa = \frac{4}{3}\left(\frac{1-\nu_1}{E_{Y1}} + \frac{1-\nu_2}{E_{Y2}}\right)^{-1} \tag{31}$$

The coefficient of dumping $b = b_f + b_m$, where

$$b_f = \frac{3\pi {d_p}^2 \mu}{2m}\left(\frac{\sqrt{k}}{2\nu}\right) \tag{32}$$

$$b_m = \frac{2.4}{\pi}\frac{mk^2}{\rho_2\left(E_{Y2}/\rho_2\right)^{3/2}} \tag{33}$$

The process of resuspension is caused by external forces, but the transmission of stress by interactions between particles is also important. Interaction between particles (or particle and collector) vanishes when the distance between their surfaces is larger than y_b.

$$y_b = 0.437\left(\frac{\pi^2\gamma^2 d_p/2}{\kappa^2}\right)^{1/3} \tag{34}$$

6. MESOSCALE INHOMOGENEITY

The first approach to modelling of mesoscale in homogeneity were purely empirical correction factors, derived to obtain agreement between theory and experiment (Benarie, 1969). These correction factors (called filter inhomogeneity factors) are defined as:

$$\Lambda_P = \frac{\Delta P}{\Delta P_{hom}} \tag{35}$$

$$\Lambda_E = \frac{ln(1-\eta)}{ln(1-\eta)_{hom}} \tag{36}$$

Cai (1992) reported the following expressions:

$$\Lambda_P = \exp\left(-3{\sigma_p}^2\right) + \frac{0.4{\sigma_p}^3}{0.8+{\sigma_p}^3} \tag{37}$$

$$\Lambda_E = \exp\left(-2{\sigma_p}^2\right) + \frac{0.8{\sigma_p}^3}{1.3+{\sigma_p}^3} \tag{38}$$

Shweers and Löffler (1994) subdivided a filter into a series of cubical elements with different local permeabilities and then used the known correlations for the single fibre deposition efficiency for each element. The distribution of local packing densities was assumed to be log-normal. The overall filter efficiency was then calculated element by element. A similar approach was used by Dhaniyala and Liu (2001). The authors also assumed log-normal distribution of local packing densities and used well known correlations to calculate single fibre efficiency as a function of the local packing density. The

Unauthenticated
Download Date | 12/15/17 11:50 AM

filter efficiency was then obtained computing the integral-mean of the deposition efficiency averaged over the assumed distribution of the packing density. An even simpler model was proposed by Clement and Dunnett (2000). The authors used the standard equation of the "classical theory", Eq. (1), assuming that for a non-uniform filter the parameter is a random variable (along various paths through a filter) having Gaussian distribution.

All these models can predict a lower pressure drop and a higher penetration than results from the "classical theory" for homogeneous structures. Neither of them, however, seems to be realistic, since they are based on the concept of the single fibre efficiency and averaging over an assumed distribution. Thus, the effect of neighbouring fibres is in practice neglected. Moreover, as the transport of aerosol in a porous space between many fibres is not considered in these models, the fundamental phenomena related to the filter non-uniformity (namely, a preferential "channelling" of flow through regions of a higher local porosity and the "shadowing" of fibres by preceding ones in zones of a lower local porosity) are not taken into consideration. Podgórski and Moskal (2001) and Podgórski (2002) have performed the analysis for a representative volume of a filter, which contains a small enough number of fibres to enable a numerical solution of microscopic transport equations, and simultaneously large enough to assure that the results obtained are statistically significant.

The model calculations consisted of the following steps: a) generation of a filtering structure consisting of 100 fibres placed in space in an assumed way (completely random distribution, perfectly regular arrangement of fibres, or a slightly disturbed ordered structure); b) characterisation of the degree of the structure inhomogeneity by dividing it into smaller parts, determination of the local packing densities and the standard deviation of the packing density distribution; c) calculation of the microscopic flow pattern in the entire structure by numerical solution of Navier-Stokes equation (using Fluent CFD package) and determination of the pressure drop; d) solution of Lagrangian transport equations (Brownian dynamics method) for a cloud of 10.000 particles injected into the filter and direct determination of the overall penetration by counting the number of particles leaving the filter; due to the stochastic nature of Brownian motion, step d) is repeated several times and results are averaged. Such simulations allow the relationships between the filter penetration, pressure drop, standard deviation of the local packing density and particle residence time to be established.

It may be concluded that classical theories of homogeneous filter media always overestimate pressure drop in real, more or less random fibrous filters. The pressure drop in a filter with a random arrangement of fibres is well correlated with the degree of filter inhomogeneity measured by the standard deviation of the local mesoscale packing density and this relationship seems to be linear.

Too high variability of the local filter porosity causes very strong channelling of the aerosol stream resulting in a drop of filtration efficiency. On the other hand when the structure becomes too regular, the shadowing effect (also lowering filtration efficiency) may be the predominant phenomenon so an optimum level of filter inhomogeneity might be expected. From the practical point of view, it seems that the bypass effect is most important for real fibrous filter structures.

Similar results were obtained by Przekop and Jackiewicz (2016). The authors studied the influence of filter inhomogeneity and fibre size distribution on deposition efficiency and pressure drop using 3D lattice-Boltzmann hydrodynamics combined with Brownian Dynamics model of particle displacement. The assumption of polydispersity of fibre sizes increased the predicted values of filtration efficiency. It was probably related to the presence of small fibres in the filter structure.

Przekop and Gradoń (2008) analysed the time evolution of quality factor defined as:

$$QF = -\frac{ln(1-\eta)}{\Delta P} \tag{39}$$

Unauthenticated
Download Date | 12/15/17 11:50 AM

for homogenous and inhomogeneous filter structures. It was shown that for inhomogeneous structures the time of filter clogging can be significantly longer than that of regular ones, so some optimum level of polydispersity not only for initial filter performance, as mentioned above, but also for its time evolution is expected.

7. DEPOSITION OF NON-SPHERICAL PARTICLES

When the transport of spherical particle is considered, it is usually sufficient to take into account only the translation of the particle mass centre. However aerosol aggregates composed of many solid particles are of great concern in most environmental issues (Wichmann and Peters, 2000). Real aggregates may undergo modifications of structure owing to the fluid–structure interaction during their movement in fluid. This fact has explicit importance in estimating aggregate deposition ratios on filter fibre. In order to establish deposition efficiencies for fractal-like aggregates, one should include interactions between primary particles which are often not stiff. Aggregate deposition efficiency is determined largely by the deformation of their structure. A flexible or rigid structure of aggregate gives different values of deposition efficiency (Podgórski et al., 1995). With the increasing power of the computers, research into the dynamics of fractal-like aggregates has been enhanced by their more complex and accurate mathematical models. There are two ways to model fractal-like aggregates. The first is to model an aggregate structure as a rigid body, which does not undergo deformation. An example of this approach can be followed in the work of Moskal and Payatakes (2006). The algorithm for the random displacement of small aggregates, whose deposition is controlled by diffusion, can be found in Bałazy and Podgórski (2007). The most important fact in this approach is that the structure and accurate shape of the aggregate are included, in order to find the real movement of the structure. The second approach allows the modelling of aggregates as flexible structures. Aggregates can be modelled with different elasticity. A common way to model an aggregate as a flexible structure is to apply interactions between primary particles, which are modelled by harmonic oscillator equation. Harmonic oscillator has been used to study the adhesion of particles on soft and rough surfaces (Reeks et al., 1988), or to model the re-entrainment of aggregates from the surface of the filter fibre (Przekop et al., 2004). This enables to go forward and use this approach to model movement of flexible aggregates in fluid. Flexible structures of aggregates, which undergo deformation under fluid interaction, are often modelled by joining together particles connected through springs or ball–socket systems. There are few examples of models of flexible aggregate structures that have been used for different tasks. Yamamoto and Matsuoka (1992) designed a flexible model consisting of connected rigid spheres, and established a new method called particle simulation method. Forces and torques acting on particles are obtained from previously calculated components of a mobility matrix. Interaction between particles is modelled by functions which mimic stretching, bending and twisting. Various structures can be analysed, such as rod-like or plate-like particles, with different abilities to deform under shear flow (Yamamoto and Matsuoka, 1999). Ross and Klingenberg (1996) used a flexible fibre model based on Yamamoto and Matsuoka's (1992) equations, where a structure is made up of rigid prolate spheroids connected through a ball and socket system. Switzer and Klingenberg (2004) developed a particle-level flexible chain fibre model, consisting of a number of cylinders connected with a ball and socket system, which has been used to investigate flocculation in the system of fibres interacting with each other. Wang et al. (2006) established a rod-chain-like fibre model, which can simulate long fibre chains with a relatively small amount of elements, which can speed up the calculations. Yamanoi and Maia (2011) analysed flexible and rigid fibres by implementing the particle simulation model approach, in order to investigate rheological properties under shear flow. In Żywczyk and Moskal (2015) model a flexible fractal-like aggregate is composed of N identical spherical primary particles. Interactions between particles are modelled by imposing equations of potential energy functions, which control stiffness of a structure. Aggregate structure is submitted to stochastic Brownian force, causing the modification of structure during its movement in fluid. The model was

Unauthenticated
Download Date | 12/15/17 11:50 AM

used to find the deposition efficiency of aggregates with different fractal dimensions, composed of various numbers of primary particles. Aggregates are conveyed towards the fibre's surface for various values of air velocity. More or less flexible structures of aggregates were analysed. It was shown that interactions between primary particles and the modifications of structure influence the efficiency of deposition of fractal-like aggregates.

8. NON-STEADY STATE FILTRATION

During an initial period of filtration, aerosol particles deposits on the collector surfaces forming chainlike agglomerates – dendrites. This phenomenon and its consequences were analysed originally for the case of submicron particles deposited on the micronsize fibres, by Payatakes and Gradoń (1980a) and then extended by Payatakes and Gradoń (1980b). The presence of previously deposited particles produces the increase of both – filtration efficiency and pressure drop. It is worth noting that not only the total amount of deposited particles, but also their spatial distribution and structure affect filter performance (Przekop and Gradoń, 2008). Most recently published papers (Karadimos and Ocone, 2003; Przekop and Podgórski, 2004; Przekop et al., 2004; Wang et al., 2006; Sztuk et al., 2012) consider particle deposition on the collector using the classical continuum approach. This approach can be efficiently used only for the initial stage of filtration, when previously deposited particles have not as yet significantly changed the fluid flow field and surface open for deposition. Some papers (Dunnett and Clement, 2006; Dunnett and Clement, 2012) take into account deposit growth, but the approach requires making assumptions of deposit structure. The important advantage in deep bed filtration modelling was the introduction of lattice gas automata (Biggs et al., 2003) and lattice-Boltzmann method (Long and Hilpert, 2009), that allows to take into account the geometry of flow change due to deposition of suspended particles. Biggs et al. (2003) have studied particle deposition in a 2D constriction unit cell and a random 2D porous medium. Long and Hilpert (2009) have studied filtration in sphere packings, using advection-diffusion equation for particle transport. By performing a set of numerical experiments the authors have developed a correlation for diffusional efficiency, but interception and sedimentation efficiency could be only obtained by employing terms from unit cell correlations. The authors have also reported numerical instabilities for fluid velocities higher than those of μm/s order.

The growth of deposits causes the decrease of local porosity and thus the increase of local fluid velocity and shear stress that may lead to the re-entrainment of single particles or aggregates. The phenomenon is not necessarily negative as resuspended particles may redeposit at the deeper layers of a filter structure, which results in a more uniform distribution of deposits through the filter and prevents the filter from clogging which boosts the filter lifetime. The combination of lattice-Boltzmann hydrodynamics, Brownian dynamics method for particle displacement and energy balanced model of adhesion, may be found as comprehensive model that may predict the nonsteady-state performance of a filter e.g. deposition efficiency, volume distribution of deposits or pressure drop (Przekop and Gradoń, 2008).

The concept of lattice applied to fluid dynamics is based on the Ulam's works on cellular automata, Ulam (1952). Fluid dynamics is especially a sufficiently large system for a cellular automaton formulation because there are two rich and complementary ways to picture fluid motion. The kinetic picture, in which many simple atomic elements rapidly collide with simple interactions, is in good agreement with the infinitive picture of dynamics in a cellular space.

The classical approach to the flow phenomena is through partial differential equations (Navier–Stokes equations) that describe collective motion in a dissipative fluid. The kinetic theory models a fluid by using an atomic picture and imposing Newtonian mechanics on the motion of the atoms.

Unauthenticated
Download Date | 12/15/17 11:50 AM

Complete information on the statistical description of a fluid at, or near, its thermal equilibrium is assumed to be contained in the one-particle phase-space distribution function f (x, t, $\Box$) for atomic constituents of the system. The variables x and t are the space and time coordinates of the atoms and $\Box$ stands for all other phase-space coordinates e.g. momentum, momentum flux. Since collisions preserve conservation laws, by integration of Boltzmann equation over the continuity equation and momentum tensor, an equation describing the macrodynamics of a system can be derived. To build a cellular-space picture with collective motion dynamics predicted by Navier-Stokes equation, a lattice on which particles move, collision rules and other restrictions characteristic for a chosen model should be defined. The evolution of the system is described by the expression:

$$f\left(\bar{x}+e_i,\bar{t}+1\right)-f\left(\bar{x},\bar{t}\right)=\Omega\left(f\right) \tag{40}$$

The outcome of a collision can be approximated by assuming that the momentum of interacting particles will be redistributed at some constant rate toward an equilibrium distribution $f_i^{eq}(x,t)$ (Qian et al., 1992). This simplification is called the single-time-relaxation approximation or lattice-BGK (Bhatnagar-Gross-Krook) and can be given by:

$$\Omega_i=\frac{1}{\bar{\tau}}\left(f_{i^{eq}}\left(\bar{x},\bar{t}\right)-f_i\left(\bar{x},\bar{t}\right)\right) \tag{41}$$

In the single-time-relaxation approximation, the momentum distribution at each lattice site is forced toward the equilibrium distribution at each time step. In the absence of external forces, the equilibrium distribution of a state with zero net momentum is just equal to momentum in each direction. The rate of change toward equilibrium is $1/\bar{\tau}$, the inverse of relaxation time, and is chosen to produce the desired value of fluid viscosity.

$$\bar{v}=\frac{\bar{c}_s{}^2}{2}\left(2\bar{\tau}-1\right) \tag{42}$$

The equilibrium distribution $f_i^{eq}(x,t)$ is given as follows:

$$f_i^{eq}=\bar{\rho}\,\alpha_i\left(1+\frac{e_i\bar{u}}{\bar{c}_s{}^2}+\frac{1}{2}\left(\frac{e_i\bar{u}}{\bar{c}_s{}^2}\right)^2-\frac{\bar{u}^2}{2\bar{c}_s{}^2}\right) \tag{43}$$

where a_i are the model dependent constants. The values of parameters in Eq. (43) for different lattice geometries can be found in Masselot (2000). The equation of state for a discrete space has the following form:

$$\bar{P}=\bar{c}_s{}^2\bar{\rho} \tag{44}$$

In traditional (continuum) flow analysis, a no-slip velocity constraint is enforced along all solid-fluid interfaces. The notion behind the no-slip condition arises from the fact that there should be no discontinuities in the velocity field within the fluid as this would give rise to infinite velocity gradients and therefore infinite shear stresses. A similar argument can be employed for conditions at the wall. However, the no-slip constraint is strictly only valid if the fluid adjacent to the surface is in local thermodynamic equilibrium; a condition which requires a very high frequency of molecular collisions with the wall. In practice, the no-slip condition is found to be appropriately provided by the Knudsen number, $Kn < 10^{-2}$. If the Knudsen number is increased beyond this value, rarefaction effects start to influence the flow and the molecular collision frequency per unit area becomes too small to ensure thermodynamic equilibrium. Under such conditions, a discontinuity in the tangential velocity will form at any solid-fluid interface.

Unauthenticated
Download Date | 12/15/17 11:50 AM

In continuum regime the bounce-back boundary condition is used on the solid level. This means that when a fluid particle enters the solid site, it changes its moving direction for the opposite one. This method naturally leads to zero-velocity at the solid level.

The model involves two parameters *r*, *s*, representing the probability for a particle to be bounced back and slipped forward, respectively. The boundary kernel takes the form, Succi (2002):

$$\mathbf{K} = \begin{pmatrix} r & 0 & s \\ 0 & r+s & 0 \\ s & 0 & r \end{pmatrix} \tag{45}$$

Obviously, the two parameters are not independent and must be chosen such that $r + s = 1$. Assuming second order slip velocity, one can write.

$$\bar{u}_{wall} = AKn\left|\frac{\partial \bar{u}_x}{\partial n}\right|_{wall} + BKn^2\left|\frac{\partial^2 \bar{u}_x}{\partial n^2}\right|_{wall} \tag{46}$$

$$A = \frac{e}{\bar{c}_s}\frac{1-r}{r}, \quad B = \frac{e^2}{\bar{c}_s{}^2} \tag{47}$$

Knudsen number for lattice is given by

$$Kn = \frac{\bar{\nu}}{\bar{c}_s \bar{d}_F} \tag{48}$$

Przekop and Gradoń (2014) have used lattice Boltzmann algorithm combined with Brownian Dynamics method for calculations of non-steady state filter performance. Aerosol particles, moving with the superficial gas velocity, were uniformly distributed at the inlet. The particles passing through the outflow surface were lost from the computational domain; while on the sides, periodic boundary conditions were applied.

The procedure of calculating numerical, dimensionless values for lattice Boltzmann model was as follows. Having assumed physical values of air velocity and fibre size, we were able to calculate Knudsen and Reynolds numbers from the definition equations. Subsequently, the value of viscosity in the attice model and then relaxation time were calculated. After that, the formula for the Reynolds number enables to calculate a dimensionless superficial velocity for lattice-Boltzmann model. The interaction between lattice-Boltzmann and Brownian dynamics may be modelled as follows. Initially, the fluid velocity profile for a clean fibre was calculated. Then, the trajectories of aerosol particles with an assumed time step were tracked. The fluid velocity in a point of space, necessary to calculate drag forces acting on a particle, was determined as a superposition from the neighbouring nodes. Obviously, the relation between dimensionless velocity in lattice Boltzmann scheme and physical one, used in Brownian Dynamics calculations, was linear. When the deposition of particle occurred, the geometry of the computational domain was changed and a new velocity profile was calculated. The similar procedure was used earlier by Filippova and Hannel (1997) and Przekop et al. (2003) for the calculation of particle deposition on single fibre or in small fibre systems.

9. SUMMARY AND OUTLOOK

A collection of aerosol particles in the particular steps of the technology of their production, and purification of the air at the workplace and atmospheric environment, requires the efficient method of separation of particulate matter from the carrier gas. Filtration is one of the effective methods for the

Unauthenticated
Download Date | 12/15/17 11:50 AM

removal of particles from an aerosol stream. The developments in the formation of specific fibrous structures promises the construction of highly efficient filters for the collection of both micro and nanoparticles. Over the last fifty years many studies on modelling of filter performance have been done. With increasing computational power of computers it became possible to overcome all the limitations of "classical theory" of filtration. Many phenomena initially predicted about filter performance were successfully explained and described at the basic level. Today, comprehensive models of deep bed filtration enable to predict filter performance evolution over time taking into account its inhomogeneous structure, particle rebound and resuspension or changes of local velocity profile due to particle deposition and dendrite growth.

SYMBOLS

A_n	complex constant of integration
AE	adhesion efficiency
b	dumping coefficient, kg/s
b_f	fluid dumping coefficient, kg/s
b_m	mechanical dumping coefficient, kg/s
B_n	complex constant of integration
$\overline{B}_n$	coupled constant of integration
C_C	Cunningham factor
$\overline{c}_s$	dimensionless sound speed
D	diffusion coefficient, m^2/s
d_F	fibre diameter, m
d_p	particle diameter, m
e	unit vector
E	single fibre efficiency
E_{BD}	single fibre efficiency interaction term
E_{det}	deterministic single fibre efficiency
E_{diff}	diffusional single fibre efficiency
E_{kp}	particle kinetic energy, J
E_R	interception single fibre efficiency
E_I	inertial single fibre efficiency
E_Y	Young's modulus, Pa
F_a	adhesion force, N
$F^{(D)}$	drag force, N
$F^{(ext)}$	external force, N
$F^{(R)}$	random Brownian force, N
G_{vi}	random number
G_{Li}	random number
J	interception coefficient
k	stiffness coefficient, kg/s^2
K_n	modified Bessel function of n-th order
Kn	Knudsen number
Ku	Kuwabara factor
L	filter thickness, m
m	mass, kg
P	pressure, Pa
$\overline{P}$	dimensionless pressure
Pe	Peclet number

Unauthenticated
Download Date | 12/15/17 11:50 AM

QF	quality factor, Pa^{-1}
r	reflection parameter
r_a	distance between atoms, m
R	interception parameter
R_K	Kuwabata cell diameter,
Re	Reynolds number
s	slip parameter
Stk	Stokes number
t	time, s
$\bar{t}$	dimensionless time
U	fluid velocity, m/s
U^*	critical fluid velocity, m/s
$\bar{u}$	dimensionless fluid velocity
v	particle velocity, m/s
x	position, m
$\bar{x}$	dimensionless position
y_b	distance between surfaces, m

Greek symbols

α	packing density
β	bounce parameter, m^2/s
β^*	critical bounce parameter, m^2/s
γ	work of adhesion, J/m^2
ε	porosity
ε_b	binding energy, J/mol
κ	elastic constant, Pa^{-1}
η	filter efficiency
Θ	angle, deg
λ	filter coefficient, m^{-1}
μ	viscosity, Pa*s
ν	Poisson's ratio
ν_f	fluid dynamic viscosity, m^2/s
$\bar{\nu}$	dimensionless viscosity
ρ_c	correlation coefficient
ρ_p	particle density, kg/m^3
$\bar{\rho}$	dimensionless density
σ	spacing between atoms at which inter-particle potential is zero, m
σ_{Li}	standard deviation of displacement, m
σ_{vi}	standard deviation of velocity, m/s
σ_p	relative standard deviation of pore size distribution
$\bar{\tau}$	dimensionless relaxation time
φ_i	distribution function
ϕ	Lennard-Jones potential, J/mol
Ω	collision term

REFERENCES

Albrecht F., 1931. Theoretische Untersuchungen über die Ablagerung von Staub aus der Luft und ihre Anwendung auf die Theorie der Staubfilter. *Physik. Zeits*., 32, 48-68.

Unauthenticated
Download Date | 12/15/17 11:50 AM

Bałazy A., Podgórski A., 2007. Deposition efficiency of fractal-like aggregates in fibrous filters calculated using Brownian dynamics method. *J. Colloid Interface Sci.*, 311, 323–337. DOI: 10.1016/j.jcis.2007.03.008.

Banks D.O., Kurowski G.J., 1990. Electrical enhancement of filters with randomly oriented fibres. *Aerosol. Sci. Tech.*, 12, 256-269. DOI: 10.1080/02786829008959344.

Benarie M., 1969. Einfluss der Porenstruktur auf den Abscheidegrad in Faserfiltern. *Staub-Reinhalt. Luft*, 29, 74-78.

Biggs M.J., Humby S.J., Buts A., Tuzun U., 2003. Explicit numerical simulation of suspension flow with deposition in porous media; influence of local flow field on deposition processes predicted by trajectory methods. *Chem. Eng. Sci*., 58, 1271-1288. DOI: 10.1016/S0009-2509(02)00103-3.

Brown R.C., 1993. *Air filtration: An integrated approach to the theory and applications of fibrous filters.* Pergamon Press, Oxford.

Cai J., 1992. *Fibrous filters with non-ideal conditions*. PhD Thesis, The Royal Institute of Technology, Stockholm.

Chandrasekhar S., 1943. Stochastic problems in physics and astronomy. *Rev. Mod. Phys*., 15, 1-89. DOI: 10.1103/RevModPhys.15.1.

Clement C.F., Dunnett. S.J., 2000. The use of random variables in fibrous filtration theory. *J. Aerosol. Sci.*, 31 (*Suppl. 1*), 200-201. DOI: 10.1016/S0021-8502(00)90207-6.

Derjaguin B.V., Muller V.M., Toporov Y.P., 1975. Effect of contact deformations on the adhesion of particles. *J. Colloid Interface Sci.* 53*,* 314-326. DOI: 10.1016/0021-9797(75)90018-1.

Dhaniyala S., Liu B.Y.H., 2001. Theoretical modeling of filtration by non-uniform fibrous filters. *Aerosl. Sci. Technol.* 34, 161-169. DOI: 10.1080/027868201300034763.

Dunnett S.J., Clement C.F., 2006. A numerical study of the effects of loading from diffusive deposition on the efficiency of fibrous filters. *J. Aerosol Sci*., 37, 1116-1139. DOI: 10.1016/j.jaerosci.2005.08.001.

Dunnett S.J., Clement C.F., 2012. Numerical investigation into the loading behaviour of filters operating in the diffusional and interception deposition regimes. *J. Aerosol Sci.*, 53, 85-99. DOI: 1016/j.jaerosci.2012.06.008.

Filippova O., Hänel D., 1997. Lattice-Boltzmann simulation of gas-particle flow in filters. *Comp. Fluids,* 26, 697-712. DOI: 10.1016/S0045-7930(97)00009-1.

Happel J., 1959. Viscous flow relative to arrays of cylinders. *AIChE J.*, 5, 174-177. DOI: 10.1002/aic.690050211.

Henry F., Ariman T., 1981. Cell model of aerosol collection by fibrous filters in an electrostatic field. *J. Aerosol Sci*. 12, 91-103. DOI: 10.1016/0021-8502(81)90041-0.

Hertz H., 1896. *Miscellaneous Papers.* Macmillan, London.

Hinds W.C., 1999. *Aerosol Technology.* Wiley & Sons, New York.

Imai I., 1951. On the asymptotic behaviour of viscous fluid flow at a great distance from a cylindrical body, with special reference to Filon's paradox. *Proc. Roy. Soc. London. Ser. A.,* 208, 487–516. DOI: 10.1098/rspa.1951.0176.

Johnson K.L., Kendall K., Roberts A.D., 1971. Surface energy and the contact of elastic solids. *Proc. R. Soc. London Ser. A,* 324, 301-313. DOI: 10.1098/rspa.1971.0141.

Karadimos A., Ocone R., 2003. The effect of the flow field recalculation on fibrous filter loading: a numerical simulation. *Powder Techn.*, 137, 109-119. DOI: 10.1016/S0032-5910(03)00132-3.

Kasper, G., Schollmeier, S., Meyer, J., 2010. Structure and density of deposits formed on filter fibers by inertial particle deposition and bounce. *J. Aerosol Sci*., 41, 1167-1182. DOI: 10.1016/j.aerosci.2010.08.006

Kirsch A.A., Fuchs N.A., 1967. Studies on fibrous aerosol filters. II. Pressure drops in systems of parallel cylinders. *Ann. Occup. Hyg*., 10, 23-30. DOI: 10.1093/annhyg/10.1.23.

Kirsch A.A., Fuchs N.A., 1968. Studies on fibrous aerosol filters. III. Diffusional deposition of aerosols in fibrous filters. *Ann. Occup. Hyg*. 11, 299-304. DOI: 10.1093/annhyg/11.4.299.

Kirsch A.A., Stechkina I.B., 1977. Inertial deposition of aerosol particles in model filters at low Reynolds numbers. *J. Aerosol Sci.*, 8, 301-307. DOI: 10.1016/0021-8502(77)90016-7.

Kuwabara S., 1959. The forces experienced by randomly distributed parallel circular cylinders or spheres in viscous flow at small Reynolds number. *J. Phys. Soc. Jpn.,* 14, 527-532. DOI: 10.1143/JPSJ.14.527.

Lamb H., 1932. *Hydrodynamics.* Cambridge University Press, Cambridge.

Lastow O., Podgórski A., 1998. Single fibre collection efficiency. In: Spurny K.R. (Ed.), *Advances in Aerosol Filtration*. Lewis Publishers, Boca Raton, 25-52.

Unauthenticated
Download Date | 12/15/17 11:50 AM

Lee K.W., Ramamurthi M., 1993. Filter collection. In: Willeke K., Baron M. (Eds.) *Aerosol Measurements: Principles, Techniques and Applications*. Van Nostrand Reinhold, New York, 188.

Lennard-Jones J.E., 1924. On the determination of molecular fields. II. from the equation of state of a gas. *Proc. Royal Soc. London A*, 106, 463-477. DOI: 10.1098/rspa.1924.0082.

Long W., Hilpert M., 2009. A correlation for the collection efficiency of Brownian particles in clean bed filtration in sphere packings by a lattice-Boltzmann method. *Eniornm. Sci. Techn.*, 35, 205-218. DOI**:** 10.1021/es8024275.

Marshall H.; Sahraoui M.; Kaviany M., 1994. An improved analytic solution for analysis of particle trajectories in fibrous, two-dimensional filters. *Phys. Fluids,* 6, 507-520. DOI: 10.1063/1.868346.

Masselot A., 2000. *A new numerical approach to snow transport and deposition by wind: A parallel lattice gas model*. PhD Thesis, Geneve University, 2000.

Maus R., Umhauer H., 1997. Single fibre collection and adhesion efficiency for biological particles. *Part. Part. Syst. Charact*., 14, 250-256.

Moskal A., Payatakes A.C., 2006. Estimation of the diffusion coefficient of aerosol particle aggregates using Brownian simulation in the continuum regime. *J. Aerosol Sci.*, 37, 1081–1101. DOI: 10.1016/j.jaerosci.2005.10.005.

Muller V.M., Yushchenko B.V. Toporov Y.P., 1980. On the influence of molecular forces on the deformation of an elastic sphere and its sticking to a rigid plane. *J. Colloid Interface Sci.* 77, 91-101. DOI: 10.1016/0021-9797(80)90419-1.

Oseen C.W., 1927. *Neuere Methoden und Ergebnisse in der Hydrodynamik.* Akademische Verlagsgesellschaft, Leipzig.

Payatakes A.C., Gradoń L., 1980a. Dendritic deposition of aerosols by convective Brownian motion diffusion for small, intermediate and large Knudsen numbers. *AIChE J.*, 26, 443-454. DOI: 10.1002/aic.690260316.

Payatakes A.C., Gradoń L., 1980b. Dendritic deposition of aerosol particles in fibrous media by inertial impaction and interception. *Chem. Eng. Sci.*, **35**, 1083-1096. DOI: 10.1016/0009-2509(80)85097-4.

Pich J.,1966. Theory of aerosol filtration by fibrous and membrane filters. In: Davies C.N. (Ed.) *Aerosol Science*, Academic Press, London, 223-285.

Podgórski A., Gradoń L., 1992. Shadow and ordering effects in fibrous electret filters. *J. Aersol Sci.,* 23 (*Suppl. 1*), 753-756. DOI: 10.1016/0021-8502(92)90521-V.

Podgórski A., 1993. Analytical description of gas flow around a fibre for modelling of aerosol filtration. *J. Aersol Sci*., 24 (*Suppl. 1*), S277-S278. DOI: 10.1016/0021-8502(93)90231-W.

Podgórski A., Gradoń L., Grzybowski P., 1995. Theoretical study on deposition of flexible and stiff fibrous aerosol particles on a cylindrical collector. *Chem. Eng. J.,* 58, 109–121.

Podgórski A., Luckner H.J., Gradoń L., Wertejuk Z., 1998. Aerosol particle filtration in the fibrous filters at the presence of external electric field I. Theoretical model. *Chem. Process Eng.*, 19, 865-889.

Podgórski A., Moskal A., 2001. Dispersion of submicron aerosol particles in fibrous filters. *Chem. Process Eng*., 22, 1139-1144.

Podgórski A., 2002. *On the transport, deposition and filtration of aerosol particles in fibrous filters: Selected problems*. Oficyna Wydawnicza Politechniki Warszawskiej, Warsaw.

Przekop R., Moskal A., Gradoń L., 2003. Lattice-Boltzmann approach for description of the structure of deposited particulate matter in fibrous filters. *J. Aerosol Sci.,* 34, 133-147. DOI: 10.1016/S0021-8502(02)00153-2.

Przekop R., Grzybowski K., Gradoń L., 2004. Energy-balanced oscillatory model for description of particles deposition and reentrainment on fibre collector. *Aerosol Sci. Techn.*, 38, 330-337. DOI: 10.1080/02786820490427669.

Przekop R., Podgórski A., 2004. Effect of shadowing on deposition efficiency and dendrites morphology in fibrous filters. *Chem. Proc. Eng.*, 25, 1563-1568.

Przekop R., Gradoń L., 2008. Deposition and filtration of nanoparticles in the composites of nano- and microsized fibres. *Aerosol Sci. Technol.*, 42, 483-493. DOI: 10.1080/02786820802187077.

Przekop R., Gradoń L., 2014. Effect of particle and fibre size on the morphology of deposits in fibrous filters. *Int. J. Num. Meth. Fluids*, 76, 779-788. DOI: 10.1002/fld.3952.

Przekop R., Jackiewicz A., 2016. Effect of filter inhomogenity on deep bed filtration process. *22nd Polish Conference of Chemical Engineering*, Spała, Poland, 5-9 September 2016, 1152-1159.

Qian Y.H., d'Humieres D., Lallemand P., 1992. Lattice-BGK models for Navier-Stokes equation. *EPL*, 17, 479–484. DOI: 10.1209/0295-5075/17/6/001.

Unauthenticated
Download Date | 12/15/17 11:50 AM

Reeks M.W., Reed J., Hall D., 1988. On the resuspension of small particles by turbulent flow. *J. Phys. D: Appl. Phys.*, 21, 574-589. DOI: 10.1088/0022-3727/21/4/006.

Ross R.F., Klingenberg D.J., 1996. Dynamic simulation of flexible fibres composed of linked rigid bodies. *J. Chem. Phys*., 106, 2949–2960. DOI: 10.1063/1.473067.

Schweers E., Löffler F., 1994. Realistic modelling of the behaviour of fibrous filters through consideration of filter structure. *Powder Technol.*, 80, 191-206. DOI: 10.1016/0032-5910(94)02850-8.

Sell W., 1931. Staubabscheidung an einfachen Körpern und Luftfiltren. *VDI Forschungs Heft.*, 347, 1-14.

Switzer L.H., Klingenberg, D.J., 2004. Flocculation in simulations of sheared fibre suspensions. *International J. Multiphase Flow*, 30, 67–87. DOI: 10.1016/j.ijmultiphaseflow.2003.10.005.

Succi S., 2002. Mesoscopic modelling of slip motion at solid-fluid interfaces with heterogeneous catalysis. *Phys. Rev. Lett.,* 89, 64502. DOI: 10.1103/PhysRevLett.89.064502.

Sztuk E., Przekop R., Gradoń L., 2012. Brownian dynamics for calculation of the single fibre deposition efficiency of submicron particles. *Chem. Process Eng.*, 33, 279-290. DOI: 10.2478/v10176-012-0025-y.

Tamada K., Fujikawa H., 1957. The steady two-dimensional flow of viscous fluid At low Reynolds number passing through an infinite row of equal parallel circular cylinders. *Q. J. Mech. Appl. Math*., 10, 425-432. DOI: 10.1093/qjmam/10.4.425.

Tomotika S., Aoi T., 1950. The steady flow of viscous fluid past a sphere and circular cylinder at small Reynolds numbers. *Q. J. Mechanics Appl. Math.*, 3, 141–161. DOI: 10.1093/qjmam/3.2.141.

Ulam S., 1952. Random processes and transformations. In: *Proceedings of the International Congress of Mathematicians (Cambridge, Massachusetts, August30-September 6, 1950),* American Mathematical Society, Providence, Rhode Island, 264-275.

Wang H.C., John W., 1987. Comparative bounce properties of particle materials. *Aerosol Sci. Technol.*, 7, 285-299. DOI: 10.1080/02786828708959165.

Wang G., Yu W., Zhou Ch., 2006. Optimization of the rod chain model to simulate the motions of long flexible in a simple shear flows. *Euro. J. Mech. B/Fluids*, 25, 337–347. DOI: 10.1016/j.euromechflu.2005.09.004.

Yamamoto S., Matsuoka T., 1992. A method for dynamic simulation of rigid and flexible fibres in a flow field. *J. Chem. Phys*., 98, 644–650. DOI: 10.1063/1.464607.

Yamamoto S., Matsuoka T., 1999. Dynamic simulation of rod-like and plate-like particle dispersed systems. *Comp. Materials Sci*., 14, 169–176. DOI: 10.1016/S0927-0256(98)00103-7.

Yamanoi M., Maia J.M., 2011. Stokesian dynamics simulations of the role of hydrodynamics interactions on the behaviour of a single particle suspending in a Newtonian fluid. Part 1. 1D flexible and rigid fibres. *J. Non-Newtonian Fluid Mech.*, 166, 457–468. DOI: 10.1016/j.jnnfm.2011.02.001.

Yeh H.C., Liu B.Y.H., 1974. Aerosol filtration by fibrous filters - I. Theoretical. *Aerosol Sci.,* 5, 191-204. DOI: 10.1016/0021-8502(74)90049-4.

Ziskind G., Fichman M., Gutfinger C., 2000. Particle behavior on surfaces subjected to external excitations. *J. Aerosol Sci*., 26, 703-720. DOI: 10.1016/S0021-8502(99)00554-6.

Żywczyk Ł., Moskal A., 2015. Modelling of deposition of flexible fractal-like aggregates on cylindrical fibre in continuum regime. *J. Aerosol Sci*., 81, 75-89. DOI: 10.1016/j.jaerosci.2014.12.002.

Received 30 November 2016
Received in revised form 10 February 2017
Accepted 11 February 2017

Unauthenticated
Download Date | 12/15/17 11:50 AM